

**Electronic Supplementary Information (ESI)**

for

**Crystal engineering by eliminating weak hydrogen**

**bonding sites in phenolic polyene nonlinear optical crystals**

O-Pil Kwon,\* Mojca Jazbinsek,\* Hoseop Yun, Jung-In Seo, Ji-Youn Seo, Seong-Ji Kwon, YoonSup Lee, Peter Günter

## 1. Synthesis

OH3 materials was prepared by Knoevenagel condensations.  $^1\text{H}$  NMR ( $\text{CD}_3\text{OD}$ ,  $\delta$ ): 2.14(2H, s, - $\text{CH}_2$ ), 2.69 (2H, s, - $\text{CH}_2-$ ), 2.79 (2H, s, - $\text{CH}_2-$ ), 6.78 (1H, s, - $\text{C}=\text{CH}-$ ), 6.78-6.81 (2H, d,  $J = 8.7$  Hz, Ar-H), 6.92-6.98 (1H, d,  $J = 18$  Hz, - $\text{CH}=\text{CH}-$ ), 7.16-7.22 (1H, d,  $J = 18$  Hz, - $\text{CH}=\text{CH}-$ ), 7.46-7.49 (2H, d,  $J = 8.7$  Hz, Ar-H).

## 2. Single crystal structure of OH3

$\text{C}_{17}\text{H}_{14}\text{ON}_2$ :  $M_r = 262.31$ , monoclinic, space group  $Cc$ ,  $a = 10.9927(8)$  Å,  $b = 12.5852(9)$  Å,  $c = 10.1326(6)$  Å,  $\beta = 94.364(2)^\circ$ ,  $V = 1397.7(2)$  Å $^3$ ,  $Z = 4$ ,  $T = 290(2)$  K, crystal dimension 0.40x0.30x0.20 mm $^3$ ,  $\mu(\text{MoK}\alpha)=0.079$  mm $^{-1}$ . Of 6705 reflections collected in the  $\theta$  range  $3.10^\circ$ - $27.5^\circ$  using an  $\omega$  scans on a Rigaku R-axis Rapid S diffractometer, 1599 were unique reflections ( $R_{\text{int}}=0.015$ , completeness=99.9 %). The C16 atom is described with a positional disorder model because of the subtle ellipsoids stretch and peaks in the difference Fourier map. The structure was solved and refined against  $F^2$  using SHELX97 [Sheldrick, G. M. (2008) *Acta Crystallogr. A64*, 112-122], 2 restraints, 192 variables,  $wR_2=0.1132$ ,  $R_1=0.0345$  ( $F_o^2 > 2\sigma(F_o^2)$ ), GOF=1.119, and max/min residual electron density 0.215/-0.107 eÅ $^{-3}$ , CCDC-682357.

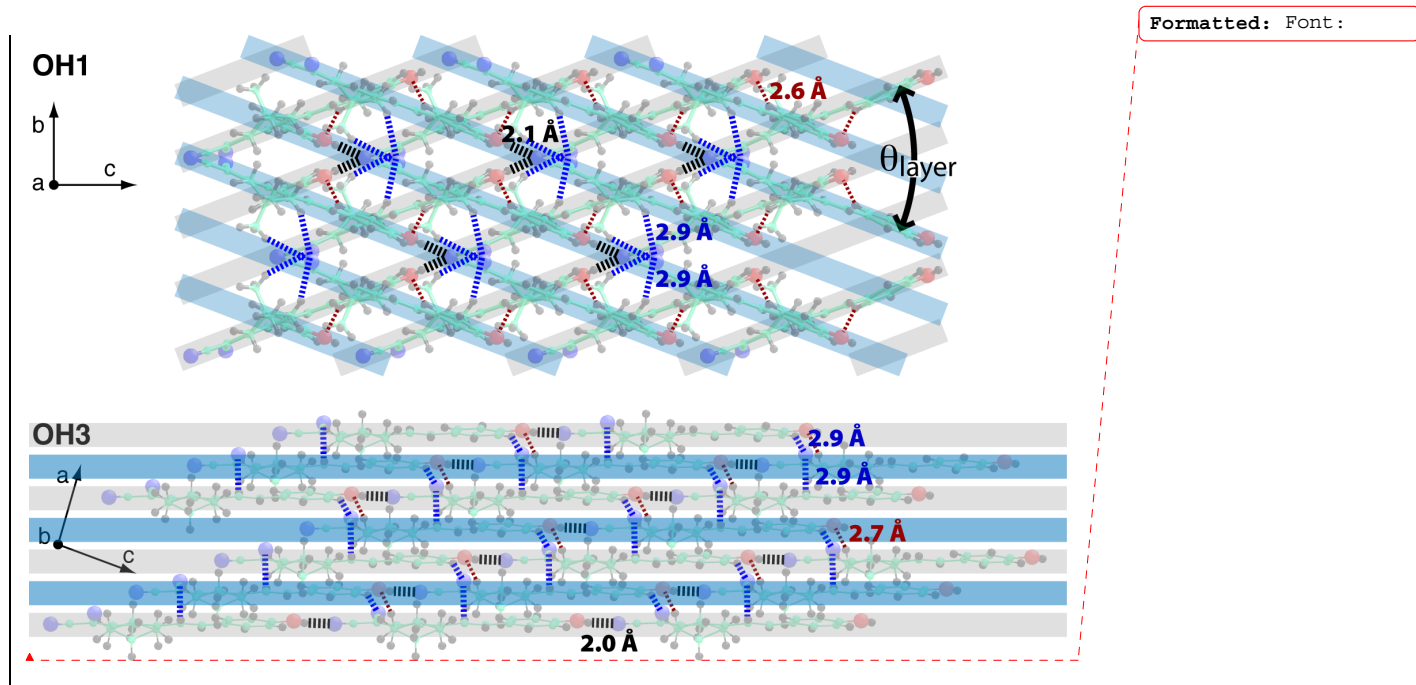


**Figure S1.** Crystal packing diagram of OH1 and OH3 crystal projected to the  $bc$  and  $ac$  crystallographic plane, respectively. The polar molecular chains (shaded) are oriented along the  $[013]$  and  $[0\bar{1}3]$  crystallographic directions in OH1, and along  $[103]$  in OH3 crystals. Main intramolecular hydrogen-bond interactions are indicated: strong  $-\text{OH} \dots \text{NC}-$  hydrogen bonds (thick black dotted lines), weak  $-\text{CH} \dots \text{NC}-$  hydrogen bonds (mid blue dotted lines), and weak  $-\text{CH} \dots \text{OH}$  hydrogen bonds (thin red dotted lines). Hydrogen bonds A-H...B indicated in this figure exhibit a bond angle between  $140^\circ$  and  $180^\circ$ .

### 3. Computational Details

#### 3.1. Microscopic Polarizabilities and First Hyperpolarizabilities $\beta$

**Table S1.** Results of the finite-field (FF) method calculated with the experimental (EXP) molecular structures determined by the X-ray diffraction analysis, at B3LYP/6-311+G\* level: dipole moments  $\mu_g$  (D), static polarizability  $\alpha_{ij}$  ( $\times 10^{-25}$  esu), the zero-frequency hyperpolarizability tensor  $\beta_{ijk}$  ( $\times 10^{-30}$  esu), the vector component  $\beta_z$  along the dipole moment direction of the hyperpolarizability tensor  $\beta_{ijk}$  ( $\times 10^{-30}$  esu), the maximal first-order hyperpolarizability  $\beta_{max}$  ( $\times 10^{-30}$  esu) and the angle  $\theta(\mu, \beta)$  (deg.) between the dipole moments  $\mu_g$  and the main direction of the first-order hyperpolarizability  $\beta_{max}$ .

	OH1 (EXP)	OH3 (EXP)
$\mu_g$ ( $= -\mu_z$ )	10.96	11.70
$\alpha_{xx}$	190.07	163.26
$\alpha_{xy}$	15.37	4.26
$\alpha_{yy}$	454.21	421.03
$\alpha_{xz}$	-10.81	-7.73
$\alpha_{yz}$	-206.12	-205.92
$\alpha_{zz}$	668.50	662.35
$\beta_{xxx}$	-0.07	-0.12
$\beta_{xxy}$	-0.23	-0.04
$\beta_{xyy}$	-1.52	-0.68
$\beta_{yyy}$	-24.31	-22.26
$\beta_{xxz}$	-0.37	-0.44
$\beta_{xyz}$	1.90	0.57
$\beta_{yyz}$	30.87	30.03
$\beta_{xzz}$	-2.30	-0.98
$\beta_{yzz}$	-35.54	-33.24
$\beta_{zzz}$	36.13	30.93
$\beta_z$	66.63	60.52
$\beta_{max}$	92.57	86.2
$\theta(\mu, \beta)$	41.6	42.4

### 3.2. Relative Second-Order Susceptibilities $\chi^{(2)}$ in the Oriented-Gas Model

The relation between the macroscopic  $\chi^{(2)}$  coefficients and the microscopic nonlinearities  $\beta$  can be estimated using the oriented-gas model [J. Zyss, J. L. Oudar, *Phys. Rev. A*, **1982**, *26*, 2028], e.g. for second-harmonic generation

$$\chi_{ijk}^{(2)}(-2\omega, \omega, \omega) = N f_i^{2\omega} f_j^\omega f_k^\omega \beta_{ijk}^{\text{eff}}(-2\omega, \omega, \omega). \quad (\text{S1})$$

The effective  $\beta_{ijk}^{\text{eff}}$  coefficients can be calculated from the hyperpolarizability tensor components  $\beta_{mnp}$  as

$$\beta_{ijk}^{\text{eff}} = \frac{1}{n(g)} \sum_s^n \sum_{mnp}^3 \cos(\theta_{im}^s) \cos(\theta_{jn}^s) \cos(\theta_{kp}^s) \beta_{mnp}, \quad (\text{S2})$$

where  $n(g)$  is the number of equivalent positions in the unit cell,  $s$  denotes a site in the unit cell, and  $\theta_{im}^s$  is the angle between the Cartesian axis  $i$  and the molecular axis  $m$ . The distinguishable components of  $\beta_{ijk}^{\text{eff}}$  in the Cartesian system are listed in Table S2 for OH1 and OH3, and were calculated by Equation (S2) considering the full three-dimensional hyperpolarizability tensor  $\beta_{ijk}$  given in Table S1. Due to the point group symmetry  $mm2$  of OH1 and  $m$  of OH3 crystals, the Cartesian system *XYZ*, in which the components in Table S2 are given, matches the crystallographic system *abc* for OH1 and is oriented as illustrated in Figure S2 for OH3 crystals.

**Table S2.** The dispersion-free components of the effective hyperpolarizability tensor  $\beta_{ijk}^{\text{eff}} \propto \chi_{ijk}^{(2)}$  ( $10^{-30}$  esu) for OH1 and OH3 in the Cartesian system *XYZ*.

OH1	$\beta_{333}^{\text{eff}}$	$\beta_{322}^{\text{eff}}$	$\beta_{311}^{\text{eff}}$		
<b>63.2</b>	7.2	8.7			
OH3	$\beta_{333}^{\text{eff}}$	$\beta_{322}^{\text{eff}}$	$\beta_{311}^{\text{eff}}$	$\beta_{133}^{\text{eff}}$	$\beta_{122}^{\text{eff}}$
<b>79.2</b>	1.2	-0.4	0.0	0.5	0.0

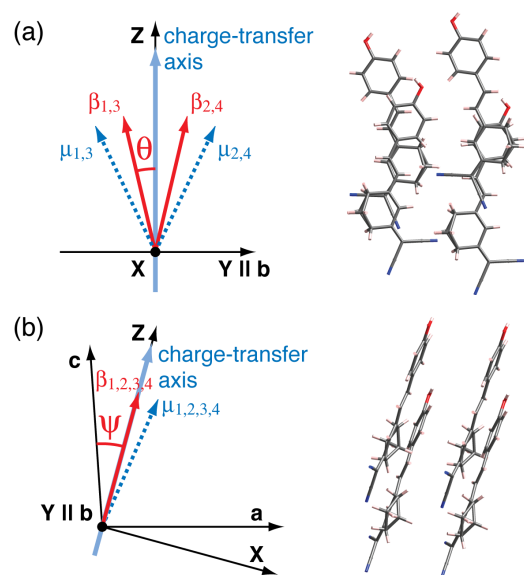


**Figure S2.** Crystal packing diagram of OH<sub>3</sub> crystals projected to the plane containing the charge transfer axis and the *b*-axis (a) and to the *ac* mirror symmetry plane (b). The angle between the main charge-transfer axis of the crystal and the hyperpolarizabilities  $\beta_{\max}$  of the molecules is  $\theta = 13.0^\circ$ . The Cartesian system *XYZ* is chosen so that *Y* is parallel to the *b* crystallographic axis and *Z* parallel to the main charge-transfer axis of the crystal, which is rotated by  $\psi \approx 20^\circ$  from the crystallographic *c* axis.